Variability of mixed radiative effect (MRE) on thin cumulus cloud

Ismail Olumegbon, Oluwafemi Akinniyi

University of Maryland Baltimore County (UMBC)

Abstract

This study highlight a new index called the mixed radiative effect (MRE) which quantifies the difference between the radiation measurements of a polluted cloud and a clean cloud. Different aerosol groups are mixed with thin cumulus cloud to form three class of polluted clouds. Their optical and radiative transfer properties are computed and compared. The biomass burning group with the highest optical depth has the highest MRE. Over the same optical depth, the urban aerosol group produce the highest MRE, thereby showing dependence on the single scattering albedo.

Introduction

There are many ways in which cloud responds to aerosol variability, hence the effect of the interaction between aerosol-cloud on radiation is difficult to understand. Twomey effect, the first indirect effect of aerosol on cloud albedo shows how an increase in CCN yields brighter clouds, with the assumption that the same amount of cloud liquid is condensed (Ian Glenn). Aside from causing brighter clouds, the interaction can have an effect on the whole lifetime of a cloud (Albrecht 1989)[3] or clouds distribution with the magnitude of all these depending on spatiotemporal analysis scale(McComiskey).

Some studies have been done on determining the aerosol radiative forcing at the top of the atmosphere using cloudy and cloud-free regions such as Feng, N., and S. A. Christopher (2015), whereby the radiative forcing is determined by the difference in the reflected radiative flux at the TOA between cloudy and cloud-free regions for anthropogenic aerosols. The radiative effect of aerosol-boundary layer cloud interaction remains a large source of uncertainty in the estimation of how the climate is sensitive to anthropogenic forcing (Boucher et al. 2013 and Glenn et al., 2020).

Monitoring of atmospheric aerosols and their interactions with clouds in the atmosphere is a tedious task. Their inhomogeneity and high variability make them very difficult to monitor. In order to explain the effects of aerosols in radiative forcing, we first determine their optical properties. Basically, these properties are aerosol optical thickness(AOT), phase function and single scattering albedo(SSA). To model the effects of atmospheric aerosols on atmospheric radiation, we solve the radiative transfer equation using aerosol optical properties. SSA determines cooling or heating effect of the aerosol radiative forcing and the magnitude of the forcing is determined by the asymmetry of the phase function and the AOT (Hansen et al., 1997). Many aerosol optical models link the optical properties of aerosols with physical and chemical characteristics of aerosols such as shape, composition and particle sizes.

In order to understand the impact of solar radiation interaction with aerosols and clouds with a view to quantifying the impact on the earth radiation budget and global climate. For aerosols, previous studies have described the aerosol radiative effect (ARE) which measures the net difference between the clear sky radiation and emitted radiation by an aerosol-laden atmosphere (Chen et. al., 2011). A positive value of the ARE is indicative of warming of the atmosphere, while a negative value signifies cooling. Similarly, the cloud radiative effect (CRE) has been equally proposed to evaluate the impact of a cloudy atmosphere over a cloud-free atmosphere (Ramanathan et al., 1989). The net radiation measurement is indicative of the CRE.

In this study, we have focused on a mixed atmosphere of aerosol and cloud with special interest on how the aerosol pollutes a clean cloud such that the mixture of aerosol with a clean cloud will yield a polluted cloud. We have proposed a new index called the mixed radiative effect (MRE), which gives the net difference between the radiation measurement of a polluted cloud and a clean cloud. As a first in this series of studies on this new index, we will have studied the simplest model possible in which only external missing is allowed and for a optically thin atmosphere. By extension, we examine the variability of different aerosol groups that mirrors practical polluted atmospheric aerosols across different geographical location

Deriving the optical and radiative properties of clean and polluted clouds

Optical properties of clean and polluted clouds

The single particle size distribution of aerosols and clouds is the precursor to determining their bulk properties. The particle size distribution for aerosols and clouds is modelled by log-normal and gamma distribution respectively. Earlier models such as Shetle and Fenn., 1979 make use of aerosol parameters such as particle size distribution, composition (complex refractive index) and shape (the deviation of aerosol particles from sphericity) (Mischenko et al. 2000). Later models have introduced more details such as internal homogeneity and complex geometric shapes. Research has shown that bimodal lognormal function is the best model for aerosol particle size distributions [2] (Whitby 1978, Remmer and Kaufmann 1998).

$$n(Inr) = \frac{dV(r)}{d\ lnr} = \frac{C_{v,f}}{\sqrt{2\pi}\sigma_f}\exp\left[-\frac{\left(lnr - lnr_{v,f}\right)^2}{2\sigma_f^2}\right] + \frac{C_{v,c}}{\sqrt{2\pi}\sigma_c}\exp\left[-\frac{\left(lnr - lnr_{v,c}\right)^2}{2\sigma_c^2}\right],$$

where C_v, r_v, and σ respectively represent the particle volume concentration, median radius, and the standard deviation for the fine (f) and coarse (c) particle sizes. The gamma distribution

$$n(r) = N_o r^{-3+v_{eff}^{-1}} \exp\left(\frac{-r}{r_{eff} v_{eff}}\right)$$

is used to model distribution of the cloud droplet in the paper with N_o, r_{eff}, v_{eff} as normalization constant, effective radius, and effective variance respectively. To model the effects of atmospheric aerosols on atmospheric radiation, we solve the radiative transfer equation using aerosol properties: phase function, aerosol optical thickness and single scattering albedo. SSA determines cooling or heating effect of the aerosol radiative forcing and the magnitude of the forcing is determined by the asymmetry of the phase function and the AOT (CF Hansen et al 1997).

Mie scattering computations are performed to determine the optical bulk properties using the following expression for the bulk single scattering albedo and phase function

$$\bar{\omega} = \frac{\int \omega(\lambda, r) Q_e(\lambda, r) \pi r^2 n(r) dr}{\int Q_e(\lambda, r) \pi r^2 n(r) dr}.$$

$$\bar{P}_{11} = \frac{\int P_{11}(\theta,\lambda,r)\omega(\lambda,r)Q_e(\lambda,r)\pi r^2 n(r)dr}{\int \omega(\lambda,r)Q_e(\lambda,r)\pi r^2 n(r)dr}.$$

As earlier defined, clean clouds are without aerosols, and polluted clouds are formed as groups of aerosol layers are externally mixed with clouds. By external mixing, there exist no physio-chemical interactions between the aerosol layer and the cloud layer. In such a simplified model, the total optical properties can be weighed by the optical depth of the interacting components $\tau_{mix} = \sum_{i=1}^{n} \tau_i$.

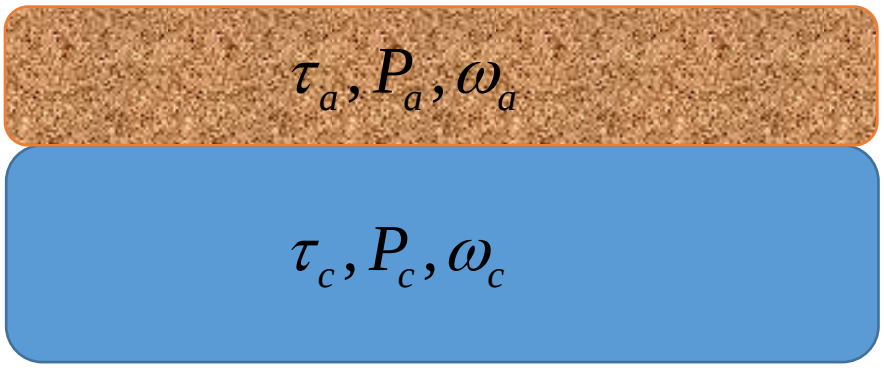

Figure 1: A layout of a typical polluted cloud showing the aerosol layer externally overlaying the cloud layer

The total optical properties (optical depth (τ), single scattering albedo (ω), and phase function (P)) of the mixture of aerosols and cloud can be deduced by using the following expression.

$$\tau_{mix} = \tau_a + \tau_c$$
$$\omega_{mix} = \frac{\omega_a\tau_a + \omega_c\tau_c}{\tau_a + \tau_c}$$
$$P_{mix} = \frac{P_a\omega_a\tau_a + P_c\omega_c\tau_c}{\omega_a\tau_a + \omega_c\tau_c}$$

Where a, c, and mix represents aerosol, cloud, and mixture respectively. The mixture of the components emeges with new optical properties different from that of the combining components.

Top of the atmosphere (TOA) radiance computation

The change in the intensity of solar radiation as it travels through the atmosphere containing clouds and aerosols in a given direction is expressed by a derivative with respect to the optical depth (τ) i.e. the rate of change of intensity with respect to the optical depth. Redirection of energy through absorption and scattering along the path of travel reduces the intensity of the travelling light. Scattering accumulated (integrated) from all directions into the direction of propagation increases the intensity. This yield the radiative transfer equation (RTE) in integro-differential form:

$$\mu \frac{\delta I(\tau,\mu,\varphi)}{\delta \tau} = -I(\tau,\mu,\varphi) + \frac{\omega_o}{4\pi} P(\mu,\mu_o,\varphi,\varphi_o) I_o \exp\left(-\frac{\tau}{\mu_o}\right) + J(\tau,\mu,\varphi)$$

$$J(\tau,\mu,\varphi) = \frac{\omega_o}{4\pi} \int_0^{2\pi} \int_{-1}^{1} P(\mu,\mu',\varphi,\varphi') I(\tau,\mu',\varphi') d\mu' d\varphi'$$

The second term in the first equation describes the first scattering of the direct solar beam Io is the TOA spectral irradiance. The solar geometry is defined by the cosine of the solar zenith angle (SZA), $\mu_o = \cos\theta_o$, and the azimuth (φ) which is assumed to be zero in the solar principal plane. By setting the J term equal to zero yields the RTE for single scattering approximation (I_1). The single scattering approximation is often treated for separately due to its analytical simplicity and importance for understanding the physics of scattering. The RTE requires two boundary condition that accounts for the incoming solar TOA and the surface reflectance at the bottom of the atmosphere. It is imposed on downward radiation at the top boundary, such that the TOA boundary condition is set to zero. In this study, we won't be considering influence of surface reflection. Also, for simplicity of the proposed problem, the single scattering approximation is applied. The RTE solution can be solved exactly to yield the expression.

$$I^{\uparrow}(TOA) = \frac{\mu_o F_o \omega_o P(\theta_s)}{4\pi} \frac{\mu_o}{(\mu_o + \mu_v)} \left[1 - \exp\left(-\frac{\tau_o}{\mu_o} - \frac{\tau_o}{\mu_v}\right)\right]$$

The effect of the surface reflectance has been neglected in this equation for the purpose of the proposed problem. The above equation written for clean and polluted clouds will have the form

$$I_{clean}{}^{\uparrow}(TOA) = \frac{\mu_o F_o \omega_c P_c(\theta_s)}{4\pi} \frac{\mu_o}{(\mu_o + \mu_v)} \left[1 - \exp\left(-\frac{\tau_c}{\mu_o} - \frac{\tau_c}{\mu_v}\right)\right]$$

$$I_{polluted}{}^{\uparrow}(TOA) = \frac{\mu_o F_o \omega_{mix} P_{mix}(\theta_s)}{4\pi} \frac{\mu_o}{(\mu_o + \mu_v)} \left[1 - \exp\left(-\frac{\tau_{mix}}{\mu_o} - \frac{\tau_{mix}}{\mu_v}\right)\right]$$

Material and experimental design

Thin Cumulus cloud

A thin layer of cumulus cloud is considered for this simplified model to allow for easy external mixing computation and single scattering approximation computation fo irradiance. A clean layer of water cloud is proposed with physical thickness of 150m, with a droplet number concentration of 100 cm^{-3} and effective radius of 5.77μm (based on information provided in the optical properties of aerosols and clouds (OPAC) database). With the extinction efficiency (Qe) obtained from the Mie-code simulation for bulk cloud properties, the optical depth (τ_c) can be computed using the expression

$$\tau_c = Q_e N_c \left(\pi r_{eff}^2\right) \Delta z$$

Aerosols groups

For effectiveness of cloud pollution by aerosol, standard aerosol combination that clearly reflect natural and anthropogenic sources from specific locations were chosen for this study. Dubovic et. al. (2000) work on the optical properties of key aerosol types observed in worldwide locations formed our source of data. Three (3) different groups were chosen as highlighted in the table below.

Groups	Aerosol type	Geographical location
Group 1	Biomass burning	African Savannah, Zambia
Group 2	Urban-industrial and mixed	GSFC, Greenbelt, Maryland, USA
Group 3	Desert, dust, and oceanic	Bahrain-Persian Gulf

Table 1: Geographical information on the aerosol groups

1. **Desert dust aerosol**

The large particles ($r > 0.6\mu m$) inherent in dust aerosol is the optical property that distinguishes it from urban-industrial aerosols.

Based on the results of many models like Koepke et al (1997), dust has albedo values lower than 0.63-0.89 at wavelength $0.5\mu m$ indicating higher absorption but because large particles dominate its distribution, ω_0 is expected to increase or be neutral. Many other studies like Carlson and Benjamin, 1980 have proven that there is low absorption in the visible to near infrared wavelengths.

Also, for the refractive index of these aerosols. In the visible spectrum, dust has a value of 1.53 for the real part of the refractive index while the value of the imaginary part is 0.08 based on many models (Shettle and Fenn, 1979). There could be slight deviations from this values however. Reports suggest that spectral dependence of the imaginary part is 3-4 times higher at the $400\mu m$ than it is at longer wavelengths.

2. **Biomass burning(BB) aerosol**

BB smoke is highly absorbing, therefore its albedo is expected to be small, but it also depends on the origin of the smoke as observed by Dubovik 2001. Their results also show that it correlates with the presence of black carbon inherent in the smoke.

The particle size distribution of smoke is in the accumulation mode, independent of region. However, the size in the accumulation mode can vary based on regions. It also follows that as a result of the accumulation mode, there is a decrease of albedo as wavelength increases and a decrease of asymmetry factor. Also, the larger the smoldering in the combustion phase, the larger the size of smoke particles.

Several studies have shown that the real part of the refractive index is in the range 1.52-1.55.

3. **Urban-Industrial aerosol**

Fine particles scattering dominates the optical properties of urban-industrial areas. Consequently, the albedo decreases, wavelength increases. The wavelength range under consideration also matters. In some wavelengths, the fine mode particles scatter radiation more than the coarse mode particles.

Experimental set-up

The set-up of the experiment is designed to mix each aerosol type with the same cloud properties in order to examine the effect and variability of their optical and radiative properties. The level and extent of their pollution will impact on their reflected radiance values at the TOA.

Groups	Aerosol type	Cloud	Label name
Group 1	No aerosol	Thin Cumulus cloud	Clean cloud
Group 2	Biomass burning	Thin Cumulus cloud	Polluted cloud I
Group 3	Urban-industrial and mixed	Thin Cumulus cloud	Polluted cloud II
Group 4	Desert, dust, and oceanic	Thin Cumulus cloud	Polluted cloud III

Table 2: different classes of clean and polluted clouds

The focus of this study is to examine the optical and radiative effect of clean cloud, and compare it with that of polluted cloud. By computing their optical properties, their variation will determine the direction of their scattering and absorption. Furthermore, the TOA radiance for the four groups is compared to highlight a net gain or loss in radiance. Lastly, we consider the different degree of predominance of the aerosol component optical depth to the net radiance increase of the polluted clouds.

Results and Discussion

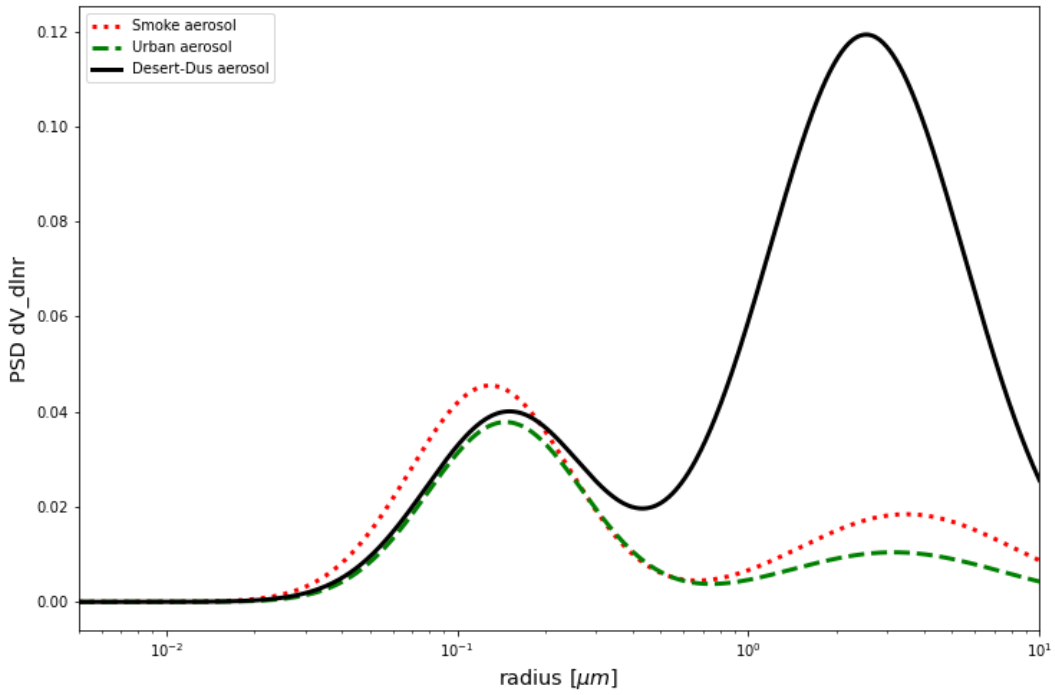

Figure 2: Comparison of the particle size distribution of the different aerosol groups.

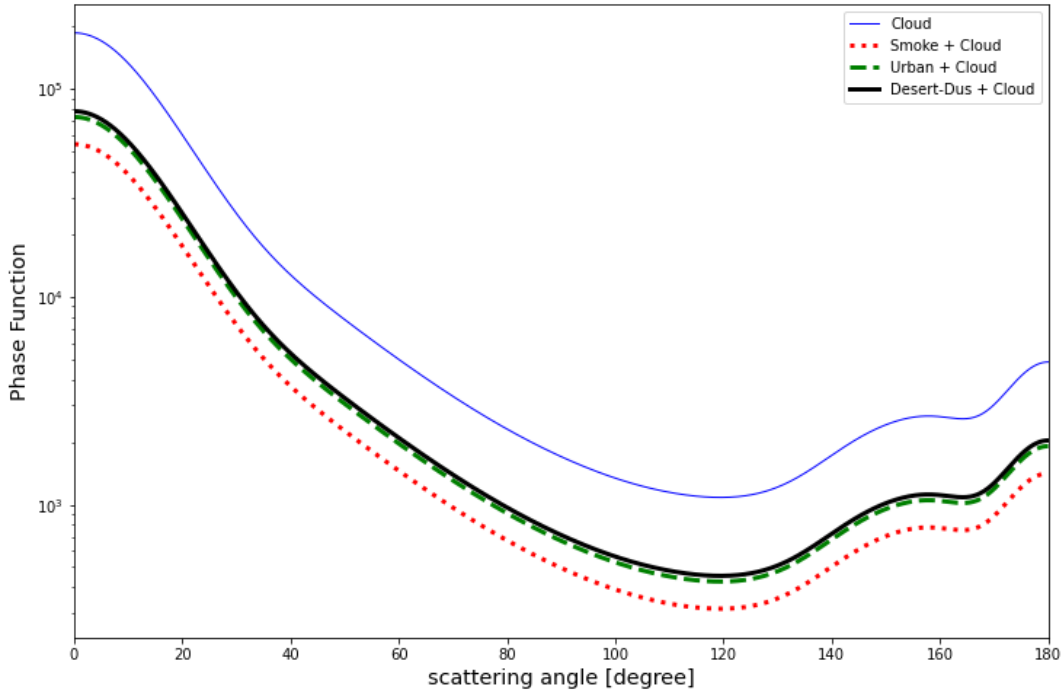

Figure 3: Comparison of the phase function of the different polluted cloud groups.

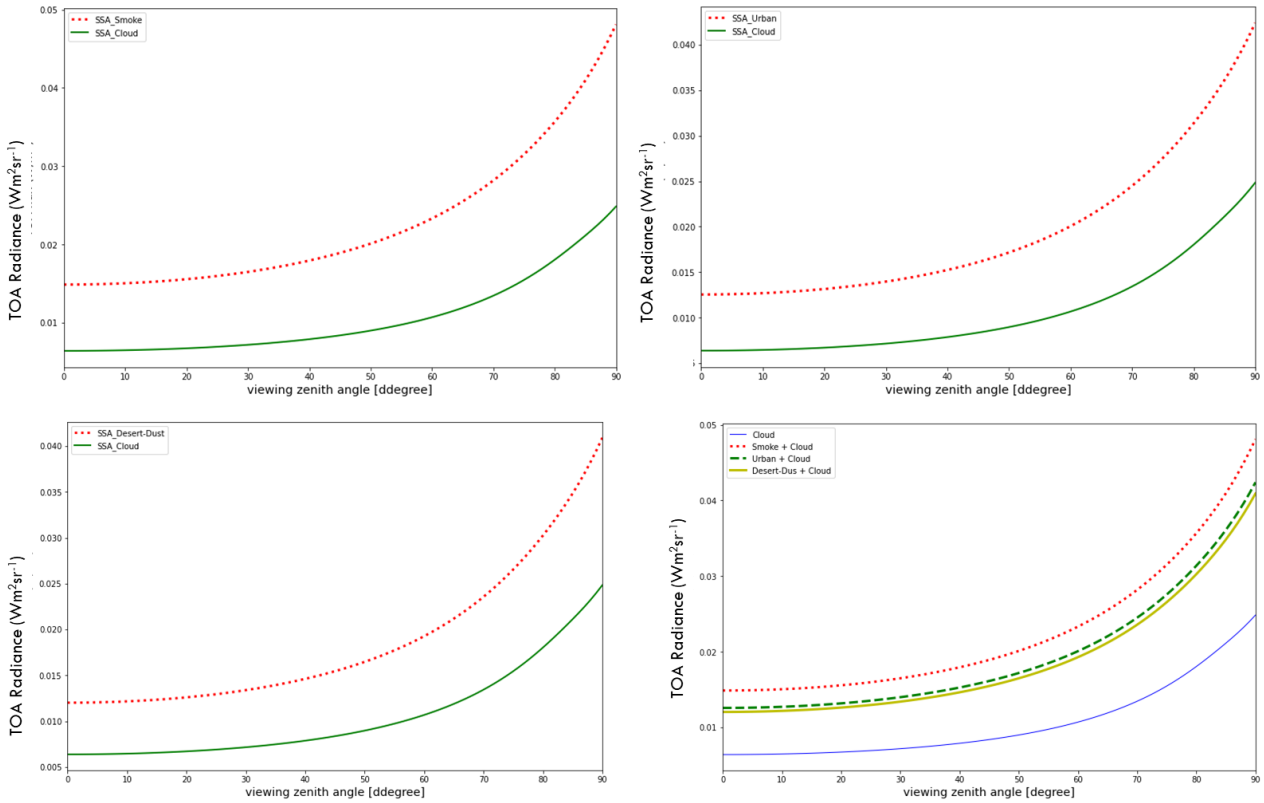

Figure 4: Comparison of the TOA radiance of the different polluted cloud groups.

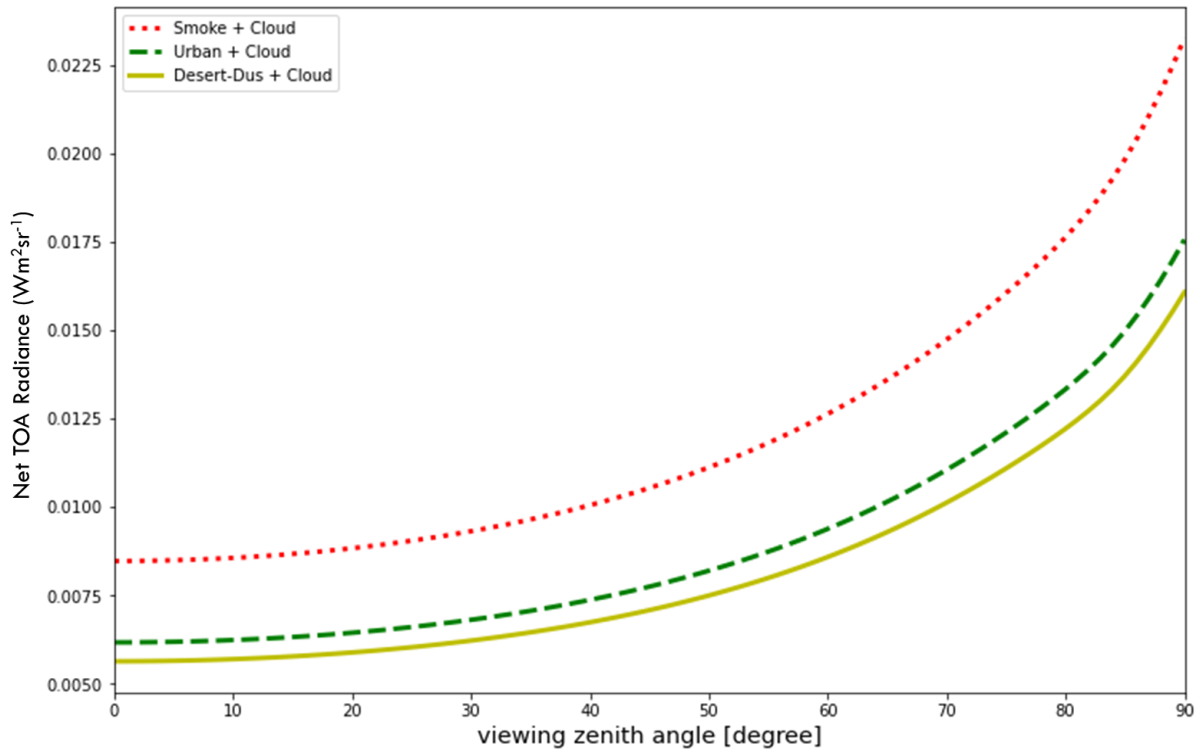

Figure 5: Comparison of the net TOA radiance of the different polluted cloud groups.

I

Groups	Aerosol type	τ	rv (f)	rv (c)	Cv (f)	Cv (c)	σ(f)	σ(c)
Group 1	Biomass burning	0.38	0.215	3.4898	0.0456	0.0342	0.4	0.74
Group 2	Urban-industrial and mixed	0.24	0.1464	3.1476	0.036	0.0196	0.38	0.75
Group 3	Desert, dust, and oceanic	0.22	0.15	2.54	0.042	0.1824	0.42	0.61

Table 3: optical and geometric information on the aerosol groups

The computation of their optical properties is a reflection of their geometrical properties. In the fine domain, smoke from biomass burning has the biggest size and the urban aerosol has the least size. This greatly impact on the cloud-albedo effect as small particle sizes has the tendency to scatter radiation more than bigger sized, and in effect improving the brightness of the cloud. This can partly explain the behaviour of the polluted group I (biomass burning + cloud) in figures 4 and 5. However, in the coarse domain shown in figure 2, the desert dust (polluted group III) shows the greatest strength in the distribution, while urban aerosol is the least in this regard. This greatly impact on absorption and explain high absorption (low albedo) of the desert aerosol group. By extension, it explain the least reflected radiance value it shows at the TOA. The dependent of the size parameter on the reflective properties of the aerosols-cloud interaction is clearly important.

Further more, to evaluate the strength of the reflected radiance for each polluted groups beyond its dependence on the optical depth. Because, the higher reflected radiance of the polluted cloud I might be entirely due to its higher optical depth. We carried out the computation of the TOA radiance for the same optical depth. Surprisingly, the urban aerosol-polluted cloud group shows the highest TOA radiance (see figure 6). No doubt, the fact that it is least dominant in the coarse domain is the major reason for this behaviour. It explains that it is the least absorption of radiation, and hence, highest scattering and single scattering albedo. This validates the dependence of scattering on the geometrical properties of the aerosol components.

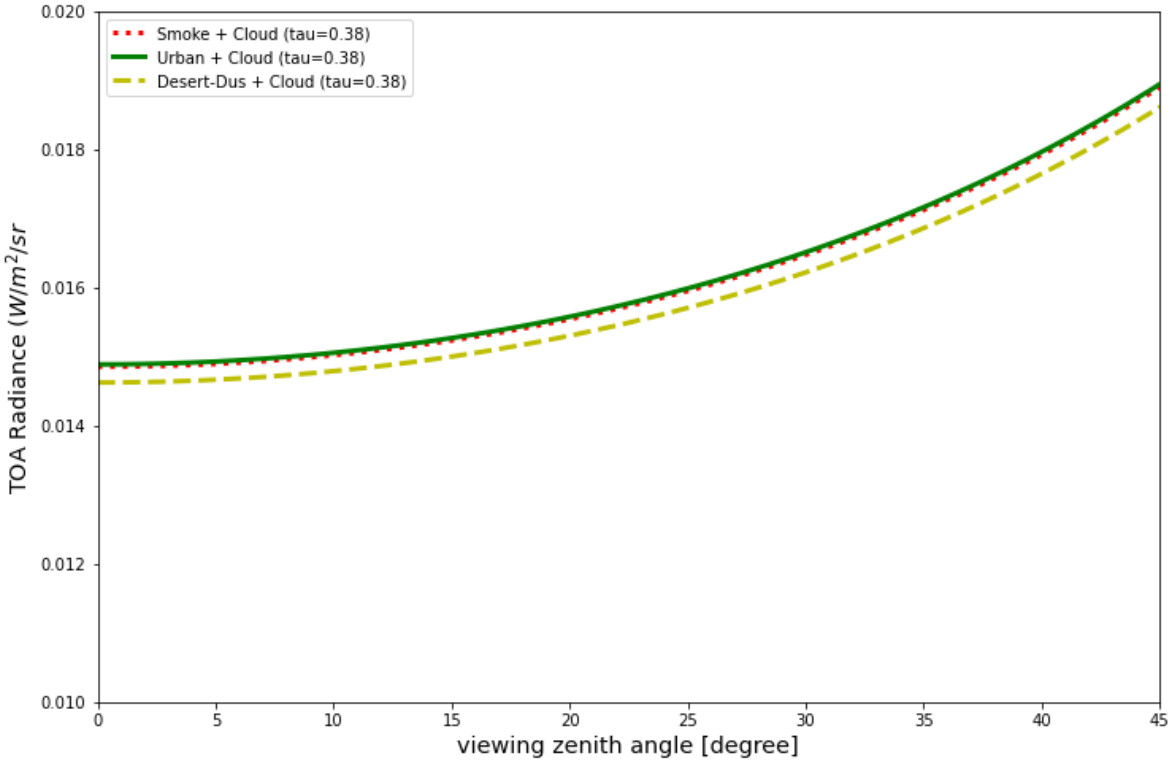

Figure 6: Comparison of the TOA radiance of the polluted cloud groups at the same optical depth.

Another important parameter that determine their overall reflective tendencies is the optical depth, as it is a measure of turbidity and attenuation coefficient of the medium. Polluted group II containing urban aerosols has the highest albedo of 0.98 as compared to 0.88 of the biomass burning aerosol, but has a lower optical depth compared to the polluted group I (biomass burning). This clearly impact on the overall reflected radiance at the TOA for the polluted group I. Figures 7 – 9 highlights the dependence of the optical depth on the reflected TOA radiance. As expected, it shows a positively linear relationship as the radiance of the increases with increase in the optical depth.

The MRE effect can be computed as the net difference between the reflected radiance of the polluted clouds and the clean cloud.

$$MRE = I_{polluted}^{\uparrow}(TOA) - I_{clean}^{\uparrow}(TOA)$$

Based on the computations the result of the MRE is highlighted in table 4 below

Groups	Aerosol type	Label name	MRE at diff τ (W/ m^2/sr)	MRE at same τ (W/ m^2/sr)
Group 1	No aerosol	Clean cloud	0	0
Group 2	Biomass burning	Polluted cloud I	0.008473229	0.008473229
Group 3	Urban-industrial and mixed	Polluted cloud II	0.006173009	0.008508042
Group 4	Desert, dust, and oceanic	Polluted cloud III	0.005638437	0.008245474

Table 2: MRE vlues for the different polluted cloud groups at nadir view (Fo = 1)

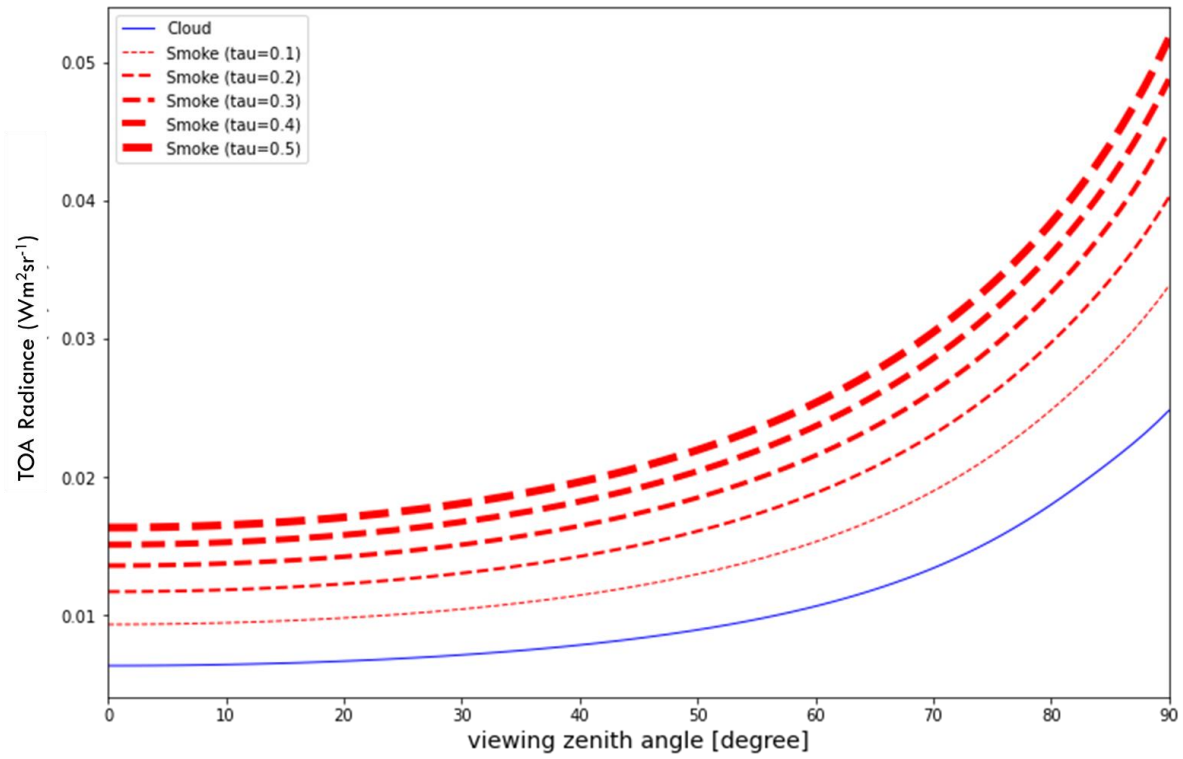

Figure 7: Comparison of the TOA radiance of the polluted cloud group I for different optical depth.

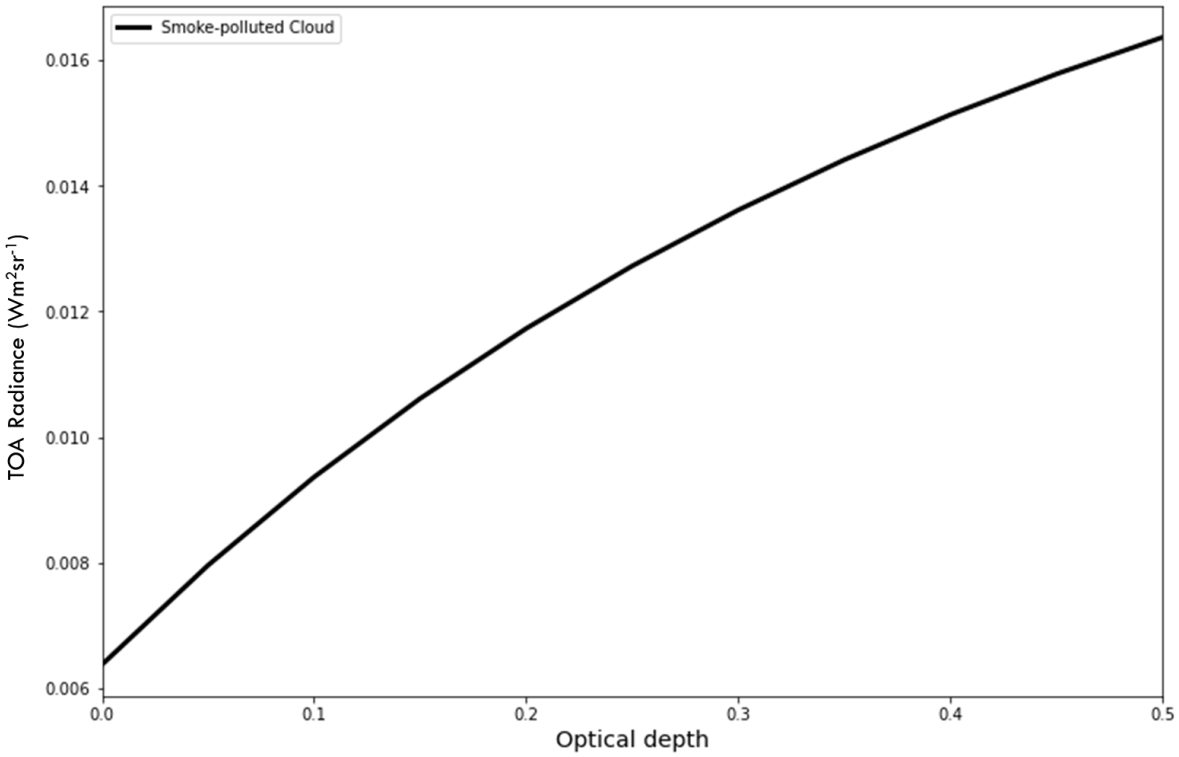

Figure 8: Variation of the TOA radiance with optical depth for the polluted cloud group I.

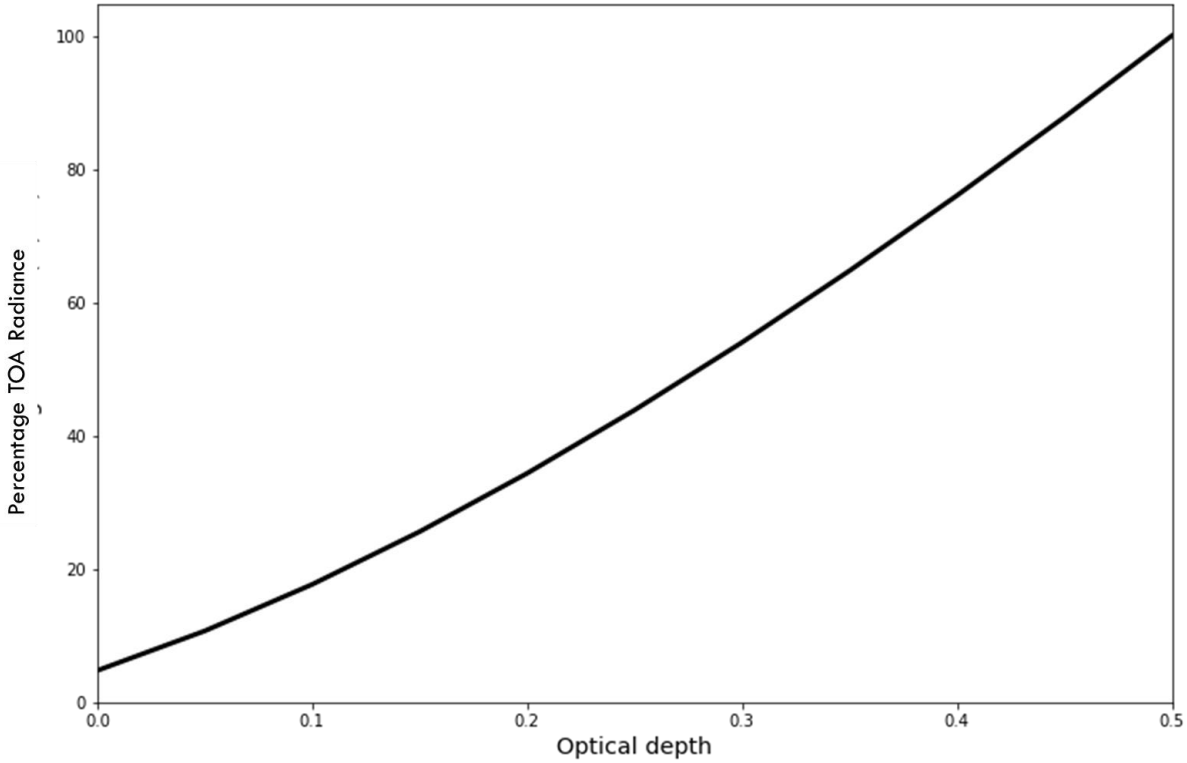

Figure 9: Percentage variation of the TOA radiance with optical depth for the polluted cloud group

Conclusion and future direction

This study highlighted the relevance of evaluating the pollution of the cloud by aerosols by considering three groups of aerosols that have been studies in the past. This study shows the strong dependence of the net TOA radiance on the optical depth as the biomass burning group with the highest optical depth reflected more than other polluted groups. However, computing the radiance of the polluted groups at the same optical depth shows the dependence of the net TOA radiance on single scattering albedo as the urban polluted groups recorded the highest reflected radiance. In general, this study emphasize the correlation of radiance with optical and geometric properties of the material medium. Finally, the notion of the mixed radiative effect (MRE) as the net radiance of the polluted clouds can help to evaluate aerosol loading and relate it as a measure of pollution.

This study leaves room for a lot of improvement as it is a simplified model and first step towards understanding pollution of the clouds. Future studies will hope to look at an optically thick atmosphere as multiple scattering will be applicable. Also, internal mixing will be considered and the net radiance and MRE can be evaluated by satellite measurement.

Reference

Albrecht, B. A., Aerosols, Cloud Microphysics, and Fractional Cloudiness. Science 1989, 245 (4923), 1227-1230.

Boucher, O., D. Randall, P. Artaxo, C. Bretherton, G. Feingold, P. Forster, V.-M. Kerminen, Y. Kondo, H. Liao, U. Lohmann, P. Rasch, S.K. Satheesh, S. Sherwood, B. Stevens, and X.Y. Zhang, 2013: Clouds and aerosols. In Climate Change 2013: The Physical Science Basis. Contribution of Working Group I to the Fifth Assessment Report of the Intergovernmental Panel on Climate Change. T.F. Stocker, D. Qin, G.-K. Plattner, M. Tignor, S.K. Allen, J. Doschung, A. Nauels, Y. Xia, V. Bex, and P.M. Midgley, Eds. Cambridge University Press, pp. 571-657, doi:10.1017/CBO9781107415324.016.

Chen, Lin, et al. "Direct radiative forcing of anthropogenic aerosols over oceans from satellite observations." Advances in Atmospheric Sciences 28.4 2011: 973-984.

Hansen, J.; Sato, M.; Ruedy, R., Radiative forcing and climate response. Journal of Geophysical Research: Atmospheres 1997, 102 (D6), 6831-6864.

Carlson, T. N., & Benjamin, S. G. Radiative Heating Rates for Saharan Dust, Journal of Atmospheric Sciences, 1980, 7(1), 193-213. Retrieved May 24, 2022

Dubovik, O. and King, D. A Flexible Inversion Algorithm for Retrieval of Aerosol Optical Properties from Sun and Sky Radiance Measurements. Journal of Geophysical Research 2000, 105, 20673-20696.

Dubovik, O.; Holben, B.; Eck, T. F.; Smirnov, A.; Kaufman, Y. J.; King, M. D.; Tanré, D.; Slutsker, I., Variability of Absorption and Optical Properties of Key Aerosol Types Observed in Worldwide Locations. Journal of the Atmospheric Sciences 2002, 59 (3), 590-608.

Glenn, I. B.; Feingold, G.; Gristey, J. J.; Yamaguchi, T., Quantification of the Radiative Effect of Aerosol–Cloud Interactions in Shallow Continental Cumulus Clouds. Journal of the Atmospheric Sciences 2020, 77, 2905-2920

Koepke, P., M. Hess, I. Schult, and E. P. Shettle, 1997: Global Aerosol Data Set. MPI Meteorologies Hamburg Report No. 243

Mishchenko, M.I., J.W. Hovenier, and L.D. Travis (Eds.), 2000: Light Scattering by Nonspherical Particles: Theory, Measurements, and Applications. Academic Press

Ramanathan, V.; Cess, R. D.; Harrison, E. F.; Minnis, P.; Barkstrom, B. R.; Ahmad, E.; Hartmann, D., Cloud-Radiative Forcing and Climate: Results from the Earth Radiation Budget Experiment. Science 1989, 243 (4887), 57-63

Remer, L.A. and Kaufman, Y.J. Dynamic aerosol model: Urban/industrial aerosol. Journal of Geophysical Research 103 1998: doi: 10.1029/98JD00994. issn: 0148-0227.

Shettle, E.P. and Fenn, R.W. Models for the Aerosols of the Lower Atmosphere and the Effects of Humidity Variations on Their Optical Properties. 1979, AFGL-TR-79-0214, 675, 94

Whitby, K. T., The Physical characteristics of Sulphur aerosols. Atmospheric Environment 1978, 12, 135-159